Design and Analysis of Microstrip Patch Antenna for WLAN and Vehicular Communication

Mandar P. Joshi[1, *] and Vitthal J. Gond[2]

Abstract—This paper presents the design and analysis of a dual-band circularly polarized (CP) microstrip patch antenna for WLAN and vehicular communication applications. In this antenna, an L-shaped slot is cut, and a square parasitic patch with diagonally opposite corners cut is loaded in offset beneath to monopole antenna to realize dual-band CP response with wideband response. The antenna exhibits dual-band CP response at 2.45 GHz (WLAN) and 5.9 GHz (Vehicular) having 20.45% and 15.73% of simulated impedance bandwidth and 6.84% and 14.16% of axial ratio bandwidth for WLAN and Vehicular band, respectively. The measured impedance bandwidth ($S_{11} < -10$ dB) is 19.43% and 12.73% for WLAN and vehicular band, respectively. The antenna design is simple and fabricated using an economical glass epoxy FR4 substrate with size of 45×40 mm². The measured results are found in good agreement with simulated results. The proposed antenna is analyzed using transmission line equivalent circuits, and the details are presented and discussed.

1. INTRODUCTION

Wireless communication applications are ubiquitous in day to day life of human beings. Many wireless communication applications empower person-to-person communication using mobile communication, and Global Positioning System (GPS) helps in location finding, Wireless Local Area Network (WLAN)/Wi-Fi services for high-speed internet access. After the tremendous growth in wireless communication, now the technology is focused towards autonomous vehicles. In July 2010, IEEE 802.11p standard for Vehicle-to-vehicle communication and dedicated short-range communication (DSRC) was developed [1]. This standard proposed new wireless communication band of 75 MHz (5.850–5.925 GHz) for Vehicle-to-vehicle (V2V) and Vehicle-to-infrastructure (V2I)/infrastructure-to-vehicle (I2V) communication [2, 3]. Recent research surveys show that the access of high speed internet in transportation systems is gaining popularity which is an emerging need of automotive industry [4–13]. The wireless access in vehicular environment (WAVE) is the future requirement of autonomous vehicle technology. Therefore, it is a great opportunity for antenna researchers to design and develop low profile antennas useful for WAVE. Microstrip patch antennas (MPAs) are advantageous as they are in low profile, easy to fabricate, and can be confirmable in size and shapes and easy to interface with RF circuitry. Recently, various researchers presented designs of microstrip antennas for vehicular communication and WAVE. A V-shaped slotted antenna with shorting pin [4], hexagon-shaped microstrip antenna for V2V communication having omnidirectional radiation pattern [5], multiband antenna for GPS, Wi-MAX and vehicular communication [6], high gain circularly polarized (CP) slotted antenna for DSRC application in [7] have been reported. A polarization reconfigurable antenna for WAVE [8], an elliptical slot loaded diagonally fed circular microstrip antenna for DSRC [9], a dual-band

[1] Department of Electronics and Telecommunication Engineering, Matoshri College of Engineering and Research Center, Nashik 422105, India. [2] Department of Electronics and Telecommunication Engineering, MET's Institute of Engineering, Nashik 422207, India.

CP antenna for GPS and DSRC applications using dual-port input in [10] have also been presented. The antennas reported in literature have complex structures, and some of the antennas reported for WAVE are linearly polarized. For vehicular communication and WAVE application, it is advantageous that antenna used in vehicle should be circularly polarized as CP antennas are immune to multipath propagation and fading. As transmitter and receiver antennas may not be perfectly aligned, CP antennas are more beneficial.

In the proposed research work, a dual-band circularly polarized low profile microstrip patch antenna having a simple structure for WLAN and vehicular communication applications is proposed. The WLAN is applicable to high speed internet access in vehicle, and vehicular communication can prevent accidents on roads. This paper is organized into five sections. The detailed geometrical structure and antenna design is presented in Section 2. The detailed transmission line equivalent circuit analysis is discussed in Section 3. The simulated and measured results are discussed and presented in Section 4, and the paper is concluded in Section 5.

2. ANTENNA GEOMETRY DESIGN

Figure 1 depicts the top and bottom sides of the proposed microstrip patch antenna. Fig. 2 represents a complete geometry of the dual-band CP antenna. The top side consists of a monopole antenna having length L_f and width of W_f. The bottom side consists of a partial ground of length L_g, an L-shaped slot having lengths L_1 and L_2, and a parasitic square patch of size $L_p \times L_p$ with cuts in diagonally opposite corners. The overall size of the used substrate is $L_s \times W_s$. In Fig. 2, the parasitic patch is in offset beneath the monopole antenna having distance 'd' between them. The detailed dimension of proposed antenna design in mm is summarized and given in Table 1.
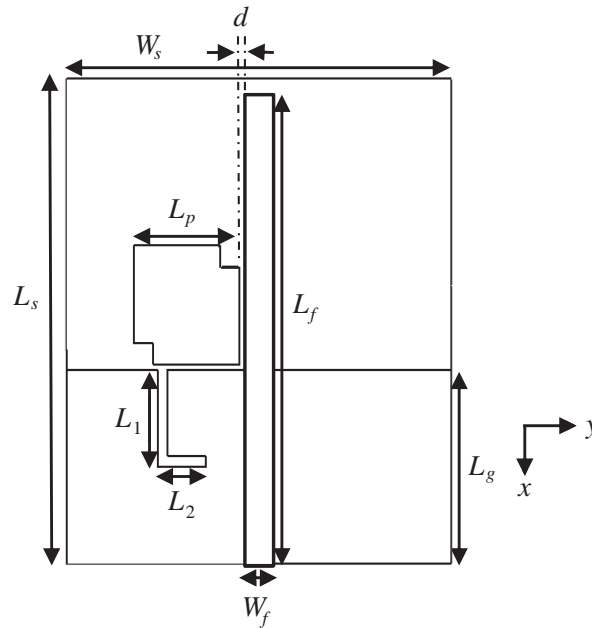
The length of monopole antenna L_f and length of partial ground L_g are optimized such that the antenna resonates at 2.45 GHz. To realize CP response, the L-shaped slot of lengths L_1 and L_2

(a)   (b)
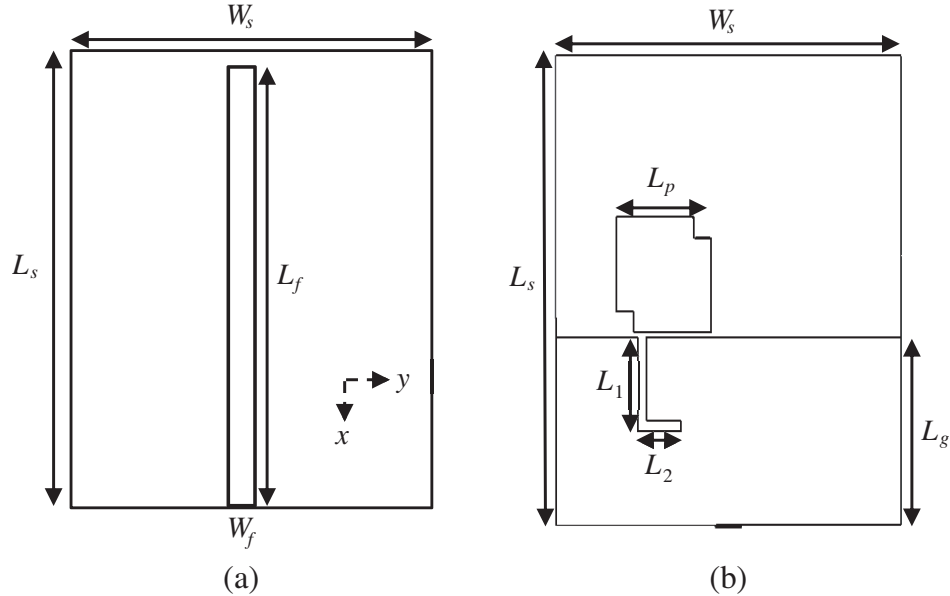
Figure 1. Geometrical structure of antenna, (a) top side, (b) bottom side.

Table 1. Dimensions of proposed antenna.

Parameter	L_s	W_s	L_f	W_f	L_1	L_2	L_g	L_p	d
Dimension (mm)	45	40	40	3	8	5	18	11	0.5

Figure 2. Complete geometry of proposed dual band CP antenna.

is cut inside partial ground. To maintain the symmetry in the L-shaped slot, slot width of 1 mm is selected. The L-shaped slot degenerates fundamental resonant mode into two degenerated modes at lower resonating frequency, to realize CP response. In order to have dual-band CP response, a square parasitic patch with diagonally opposite corners cut has been designed and placed in offset beneath monopole antenna. The length of the parasitic square patch is calculated using Equation (1) [14].

$$L_p \approx \frac{c}{2f_r\sqrt{\varepsilon_r}} \tag{1}$$

where c is 3×10^8 m/s; ε_r is the relative permittivity of substrate used; and f_r is the desired resonant frequency. Length L_p of parasitic square shaped patch is calculated for desired resonant frequency at 5.9 GHz. To exhibit CP response at higher frequency, the diagonally opposite corners of square patch antenna are cut in the size of 2×2 mm^2. The offset beneath distance of parasitic square patch with respect to top side monopole is optimized at dimension 'd'. The novelty of this research work is that it offers independent tuning at lower and higher resonating frequencies, which is discussed in results. The realized CP results can be independently tuned by varying length of the L-shaped slot and distance 'd' of parasitic square patch with respect to monopole for lower and higher resonant frequencies, respectively. An economical glass epoxy FR4 substrate having parameters $h = 1.6$ mm, $\varepsilon_r = 4.3$, and $\tan\delta = 0.02$ is used to fabricate the proposed antenna. A standard SMA connector is used to feed the antenna. The designed antenna is simulated using method of moments, and Altair's CAD FEKO is used as an antenna simulator [15]. In next section, theoretical discussion on transmission line equivalent circuit analysis is presented in detail.

3. THEORETICAL DISCUSSION AND EQUIVALENT CIRCUIT ANALYSIS

The theoretical analysis of proposed antenna has been carried out by equivalent circuit theory method. The entire geometry of antenna can be divided in to three subsequent sections viz. (i) microstrip line as resonator, (ii) analysis of L-shaped slot, and (iii) analysis of parasitically coupled square patch.

3.1. Microstrip Line as Resonator

The microstrip line on the top of substrate is designed to act as a monopole antenna having length equal to quarter wave at desired lower resonant frequency. Width W_f is calculated to match input impedance

of antenna at $50\,\Omega$ [16]. As the microstrip line acts as a resonator, it can be modelled and represented as parallel R, L, C circuit. These lumped parameters can be calculated and given by [17].

$$C_1 = \frac{2w_f \varepsilon_r}{L_f h \omega_0^2} \tag{2}$$

$$L_1 = \frac{1}{C_1 \omega_0^2} \tag{3}$$

$$R_1 = \frac{Q}{\omega_0^2 C_1} \tag{4}$$

In Equations (2), (3), and (4), L_f and w_f are the length and width of monopole antenna, respectively; h is the substrate thickness in mm; ω_0 is the angular frequency; and Q is the quality factor as given in [18].

$$Q = \frac{c\sqrt{\varepsilon_{re}}}{4f_r h} \tag{5}$$

where ε_{re} is the effective dielectric constant of substrate and calculated using Equation (6) [18].

$$\varepsilon_{re} = \frac{(\varepsilon_r + 1)}{2} + \frac{(\varepsilon_r - 1)}{2\sqrt{1 + 12\dfrac{h}{w_f}}} \tag{6}$$

The estimated values of L_1 and C_1 are $2.48\,\text{mH}$ and $1.70 \times 10^{-18}\,\text{F}$, respectively. The microstrip line as a resonator is modelled as parallel R_1, L_1, and C_1 and depicted in Fig. 3.
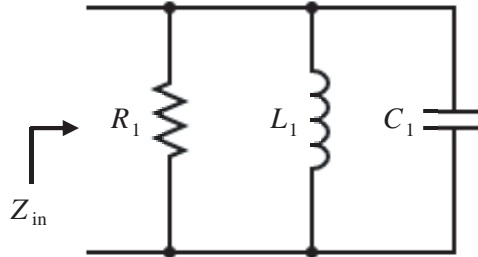
Figure 3. Equivalent circuit of monopole antenna.

3.2. Analysis of L-Shaped Slot

An L-shaped slot is cut across the edge of ground plane to degenerate the fundamental resonant mode into two degenerative modes to realize CP response at lower frequency. The L-shaped slot has the total length of L' given in Equation (7).

$$L' = L_1 + L_2 \tag{7}$$

where L_1 and L_2 are lengths of the L-shaped slot. This cutting of slot creates a gap between two conducting planes in ground plane and forms a capacitance, and slot length L' forms an inductance. This can be attributed by adding a series capacitance ΔC and series inductance ΔL into C_1 and L_1, respectively. The modified inductance and capacitance are L_2 and C_2, respectively. The modified equivalent circuit is shown in Figs. 4(a) and (b). The values of L_2 and C_2 can be estimated as [19].

$$L_2 = L_1 + \Delta L \tag{8}$$

$$C_2 = \frac{C_1 \Delta C}{C_1 + \Delta C} \tag{9}$$
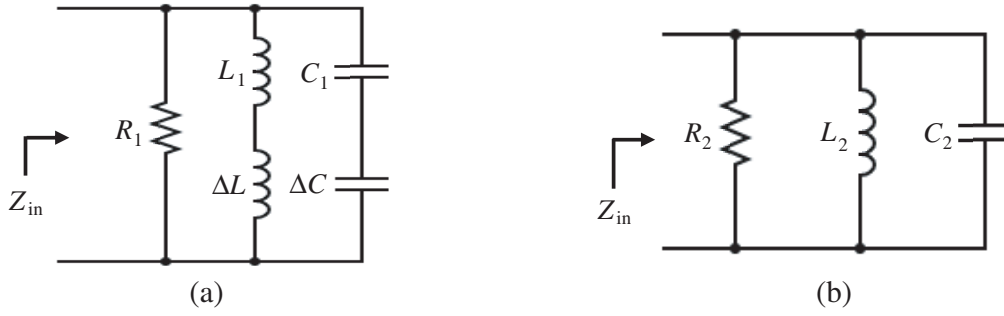
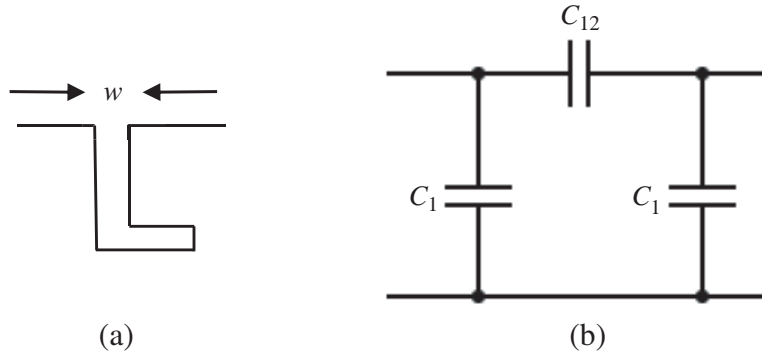**Figure 4.** (a) Series inductance and capacitance, (b) modified equivaled circuit.

Figure 5. (a) L-shaped slot in ground plane, (b) equivalent capacitance of L-shaped slot.

where,

$$\Delta L = \frac{h \mu_0 \pi}{8} \left(\frac{L'}{w} \right) \tag{10}$$

In Equation (10), $\mu_0 = 4\pi \times 10^{-7}$ H/m, L' is the total slot length, w the width of slot, and h the substrate thickness in mm. The gap formed by the L-shaped slot can be modelled in the form of terminal capacitance C_1 and gap capacitance C_{12} as represented in Fig. 5 [18].

This terminal and gap capacitance is divided into two capacitances, namely even and odd, and expressed as [18].

$$C_1 = \frac{1}{2} \text{even} \tag{11}$$

$$C_{12} = \frac{1}{2} \left(C_{\text{odd}} - \frac{1}{2} C_{\text{even}} \right) \tag{12}$$

$$\frac{C_{\text{odd}}}{w} = \left(\frac{s}{w} \right)^{\left\{ \frac{w}{h} \left(0.619 \log \frac{w}{h} - 0.3853 \right) \right\}} \exp \left(4.26 - 10453 \log \frac{w}{h} \right) \tag{13}$$

$$\frac{C_{\text{even}}}{w} = \left(\frac{s}{w} \right)^{0.8675} \exp \left(2.043 \left(\frac{w}{h} \right)^{0.12} \right) \tag{14}$$

$$C_{\text{even}} \left(\varepsilon_r \right) = C_{\text{even}} \left(9.6 \right) \left(\frac{\varepsilon_r}{9.6} \right)^{0.9} \tag{15}$$

$$C_{\text{odd}} \left(\varepsilon_r \right) = C_{\text{odd}} \left(9.6 \right) \left(\frac{\varepsilon_r}{9.6} \right)^{0.8} \tag{16}$$

Capacitance ΔC can be calculated from Equations (11) to (16) and found as 3.09 pF. Substituting the value of ΔC in Equation (9) yields $C_2 = 1.69 \times 10^{-18}$ F. The new resonance frequency calculated using $L_2 = 2.48$ mH and $C_2 = 1.69 \times 10^{-18}$ F is 2.45 GHz. These calculations verify that the newly calculated

values of inductance and capacitance do not change the lower resonance frequency. The L-shaped slot neither changes the performance of monopole antenna nor alters the lower resonance frequency. It solely degenerates fundamental lower frequency into two frequency components of same amplitude and phase quadrature, realizing CP response.

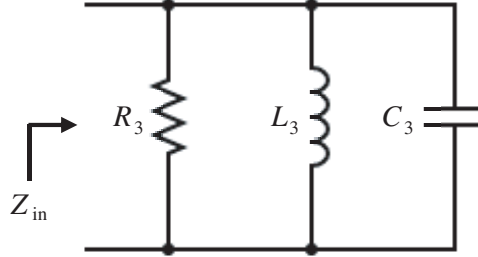### 3.3. Analysis of Parasitically Coupled Square Patch

The square patch of length L_P, calculated using Equation (1), is placed in offset beneath monopole antenna to resonate at vehicular communication frequency of 5.9 GHz. This patch is parasitically coupled and excited by the fringing fields of monopole antenna. This patch can also be modeled as parallel R, L, C network and given as [18].

$$C_3 = \frac{\varepsilon_0 \varepsilon_r LW}{2h} \cos^{-2}\left(\frac{\pi y_0}{L}\right) \tag{17}$$

$$L_3 = \frac{1}{\omega_0^2 C_3} \tag{18}$$

$$R_3 = \frac{Q}{\omega_0^2 C_3} \tag{19}$$

In Equations (17)–(19), L and W are the length and width of microstrip patch, respectively; y_0 is the feed location; ω_0 is the angular frequency; ε_r is the dielectric constant of substrate; h is the substrate thickness; $\varepsilon_0 = 8.854 \times 10^{-12}$ F/m. The estimated values of inductance and capacitance using Equations (17) and (18) are 0.50 nH and 1.43 pF, respectively. The equivalent circuit of parasitically coupled microstrip patch is depicted in Fig. 6.

Figure 6. Equivalent circuit of square patch.

As this square patch is excited by fringing fields of monopole antenna, there exists a fringing capacitance between monopole antenna and parasitically coupled square patch. This fringing capacitance can be calculated using Equations (20)–(21) [18].

$$2C_f = \sqrt{\frac{\varepsilon_{re}}{c \cdot Z_0}} - C_p \tag{20}$$

$$C_p = \varepsilon_0 \varepsilon_r \frac{w}{h} \tag{21}$$

In Equations (20) and (21), C_p is the parasitic capacitance and estimated using Equation (21). w is the width of monopole antenna, h the substrate thickness, Z_0 the characteristics impedance, and ε_{re} the effective dielectric constant estimated using Equation (6). The estimated value of fringing capacitance is 7.35 μF. The complete transmission line equivalent circuit of dual-band antenna is presented in Fig. 7.

4. RESULTS AND DISCUSSION

4.1. Simulation Results

The simulated return loss characteristics, axial ratio, and surface current distribution at 2.43 GHz of monopole antenna with an L-shaped slot in ground are depicted in Fig. 8.
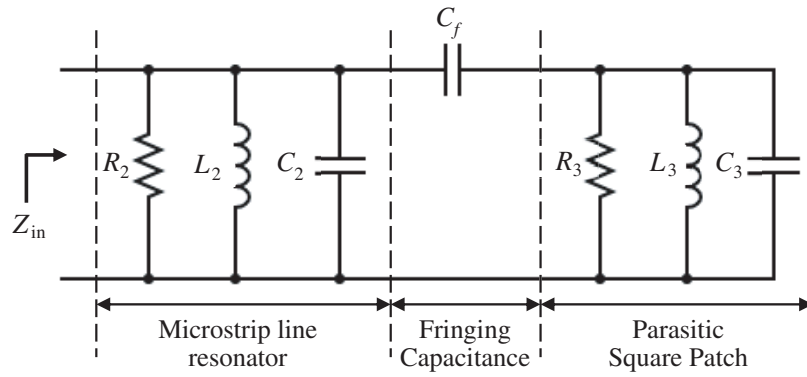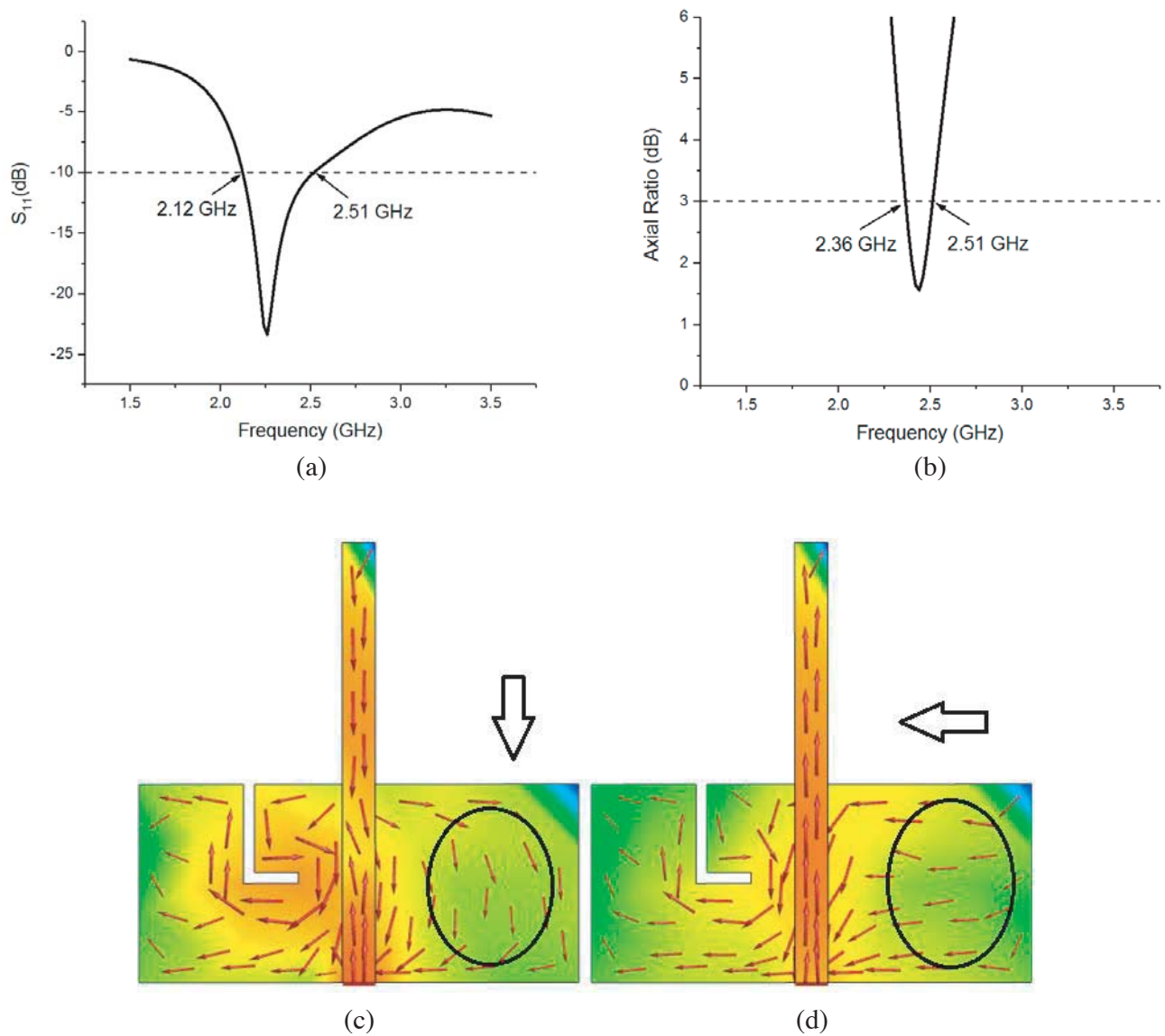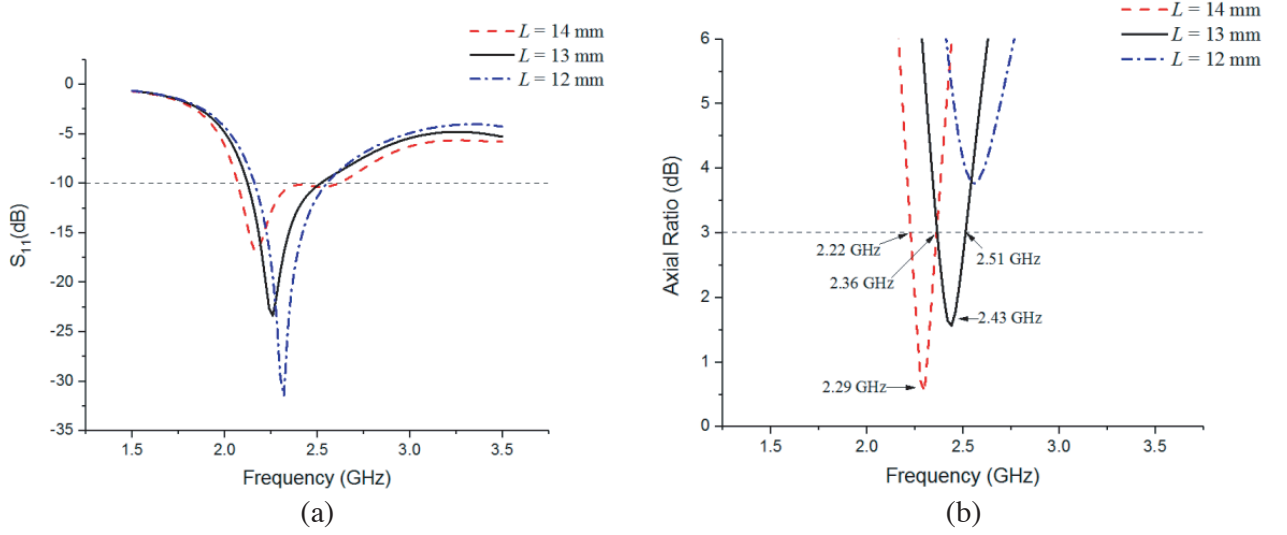
Figure 7. Equivalent circuit of dual band MPA.

(a)

(b)

(c)   (d)

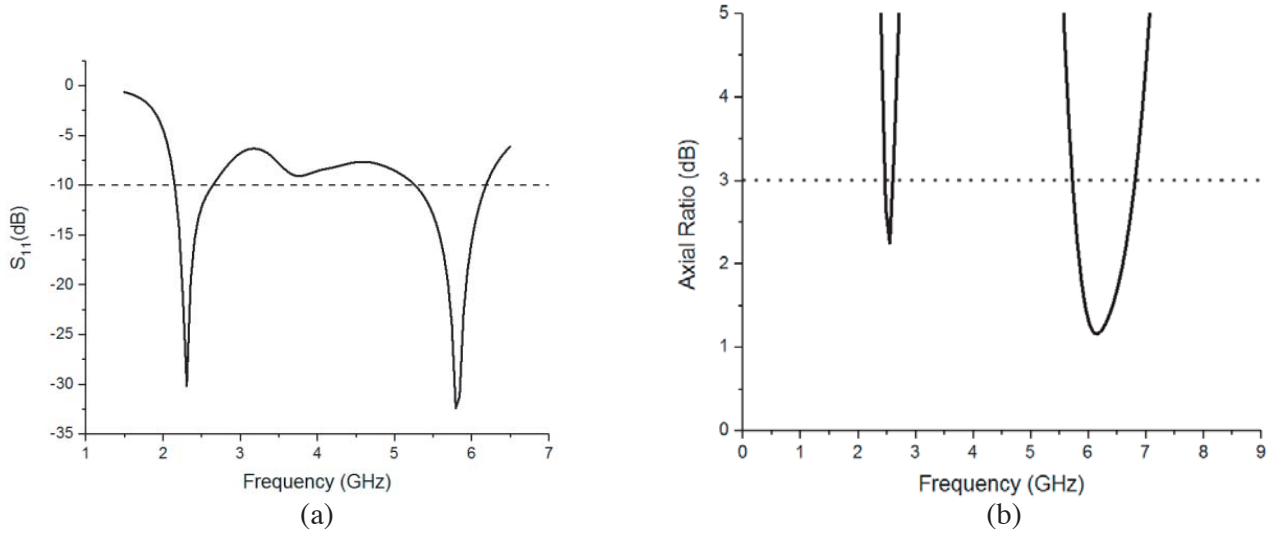**Figure 8.** Simulated L-shaped slotted CP monopole antenna, (a) return loss characteristics, (b) axial ratio, (c) surface current at 0°, (d) surface current at 90°.

Figure 9. Effect of variation of length L of L-shaped slot on (a) return loss, (b) axial ratio.

Figure 10. Simulated characteristics of dual band CP antenna, (a) return loss, (b) axial ratio.

As presented in Fig. 8(a), the realized impedance bandwidth $< -10\,\text{dB}$ is 16.84% covering lower WLAN/Wi-Fi wireless communication band. The L-shaped slot realized CP response and offers 6.16% of axial ratio bandwidth as given in Fig. 8(b) with a gain of 1.48 dBi. Figs. 8(c) and (d) show surface current at 2.43 GHz for 0° and 90°, respectively. As shown in Figs. 8(c) and (d), it is verified that the proposed monopole antenna is left hand circularly polarized (LHCP) in lower band of application, as direction of current is in clockwise. The axial ratio of the monopole antenna can be tuned to lower resonant frequency by varying the length of the L-shaped slot. The variation in length of the L-shaped slot is studied, and the effects on return loss and axial ratio characteristics are shown in Fig. 9.

The total length of the L-shaped slot is taken equal to quarter wavelength at lower resonant frequency and calculated using Equations (22) and (23).

$$L = L_1 + L_2 \approx \frac{\lambda_g}{4} \tag{22}$$

$$\lambda_g = \frac{\lambda_0}{\sqrt{\varepsilon_{re}}} \tag{23}$$

As depicted in Fig. 9(a), varying the total length of L-shaped slot changes resonant frequency and impedance bandwidth of monopole antenna. It is observed that lowering the length of slot shifts resonant frequency to higher side with impedance bandwidth of 15.77%, while higher value of slot shifts resonant frequency to lower side with impedance bandwidth of 23%. This is because length of L-shaped slot modifies the length of current in the ground plane. Though the impedance bandwidth has been increased, this change in length shows vital impact on axial ratio bandwidth. From Fig. 9(b), it is observed that the change on slot length affects axial ratio and axial ratio bandwidth. For higher value of slot length, axial ratio shifts to lower side and resonates at 2.29 GHz having axial ratio bandwidth from 2.22 to 2.36 GHz, which is not desired lower WLAN band. For lower value of slot length, axial ratio becomes > 3 dB. Therefore, the total length of L-shaped slot has been optimized at $L = 13$ mm. To realized dual-band CP antenna, a square patch with diagonally opposite corners cut is placed offset beneath with respect to monopole. This patch resonates at 5.9 GHz vehicular band having 15.73% and 14.16% of impedance and axial ratio bandwidth, respectively. The return loss and axial ratio characteristics are shown in Fig. 10.

The dual-band antenna covers impedance bandwidth from 2.15 to 2.64 GHz (20.45%) and axial ratio bandwidth of 2.4–2.57 GHz (6.84%) for lower band, 5.27–6.18 GHz (15.73%) of impedance bandwidth, and 5.64–6.5 GHz (14.16%) of axial ratio bandwidth for higher band, respectively. It is also observed that
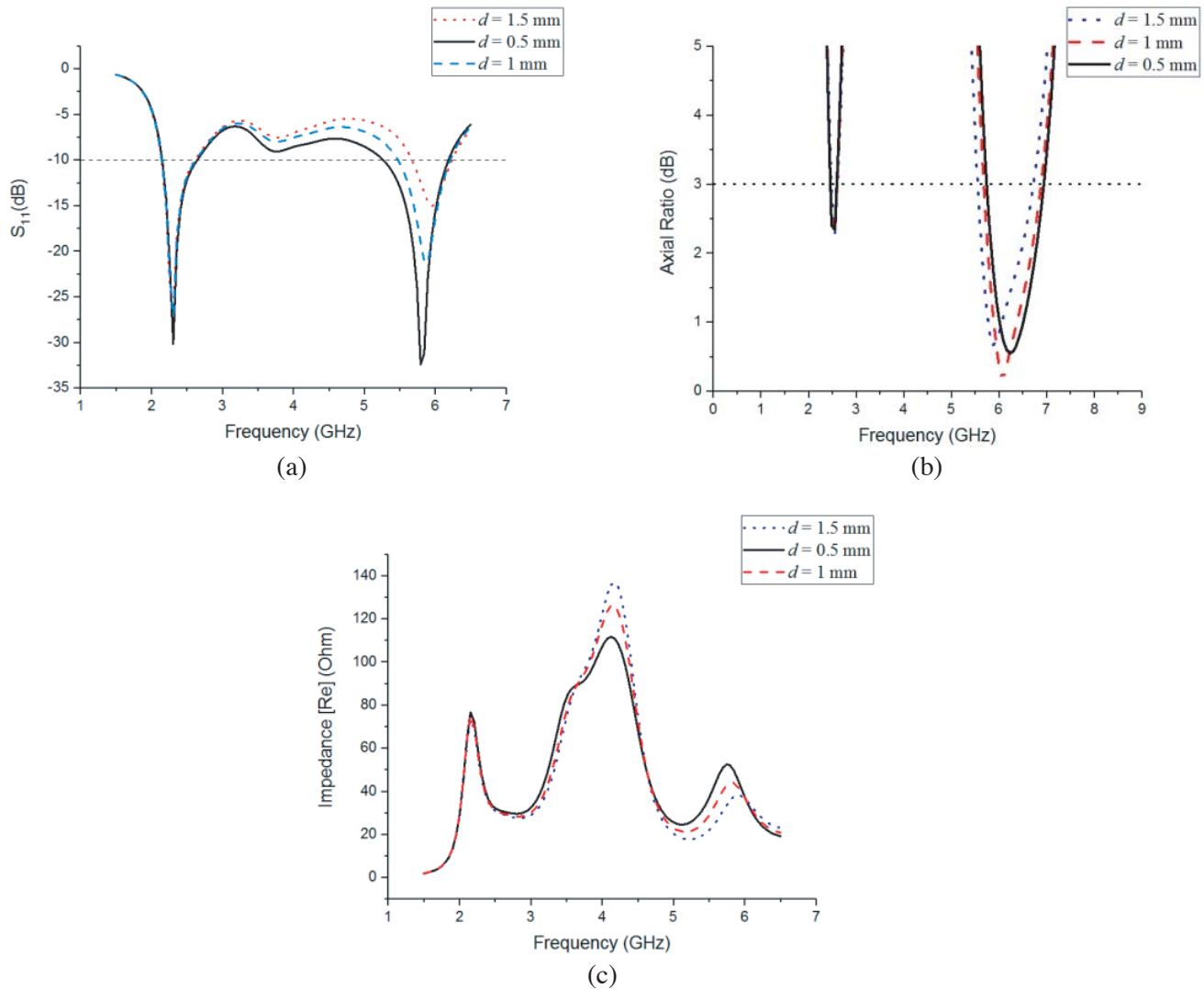
Figure 11. Effect of variations in distance 'd' on (a) return loss, (b) axial ratio and (c) impedance.

higher frequency band having 860 MHz axial ratio bandwidth covers vehicular communication (5.850–5.925 GHz), higher WLAN (5.725–5.825 GHz), and Wi-MAX (5.64–5.85 GHz) wireless communication applications. The effect of parasitic patch placed in offset beneath is also studied, and it is observed that the distance between parasitic patch and monopole has significant effect on the performance of antenna. The effects on return loss, axial ratio, and impedance characteristics by varying distance '*d*' are shown in Fig. 11.

It is observed that by varying distance '*d*', higher frequency band can be tuned independently without altering the performance of lower frequency band. By varying the distance, better axial ratio performance < 3 dB has been observed as shown in Fig. 11(b). However, this variation leads to change in impedance value and impedance bandwidth as shown in Figs. 11(c) and (a), respectively. This variation
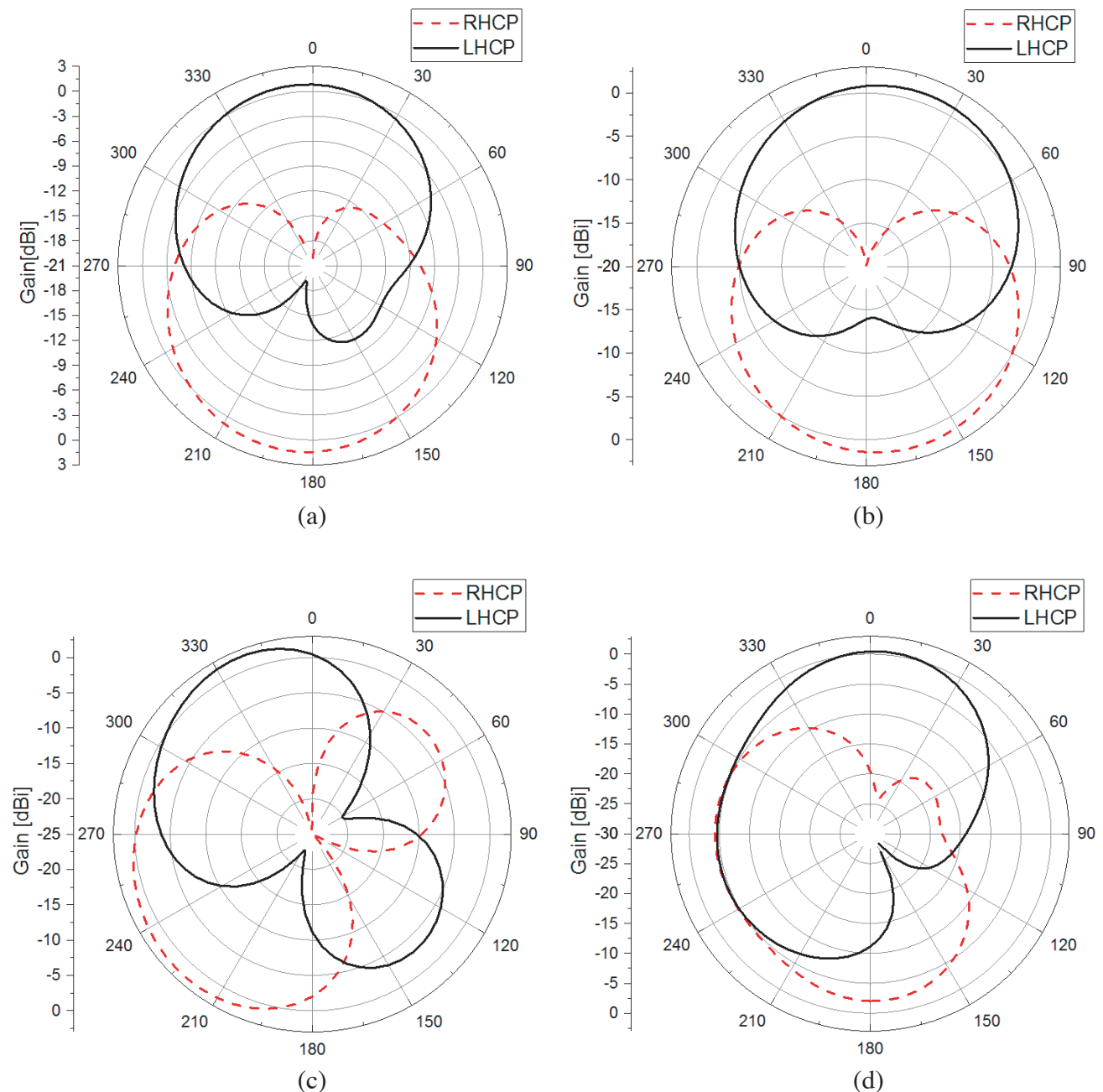

Figure 12. Radiation pattern at 2.45 GHz (a) *E*-plane, (b) *H*-plane, 5.9 GHz, (c) *E*-plane, (d) *H*-plane.

in 'd' limits the impedance bandwidth of higher resonating band which yields narrow band response.

Figures 12(a) and (b) show E-plane and H-plane radiation patterns at 2.45 GHz, and (c) and (d) show E- and H-plane patterns at 5.9 GHz. The simulated peak CP gains at 2.45 GHz and 5.9 GHz are 1.48 dBi and 1.95 dBi, respectively. The antenna exhibits LHCP in $+z$ direction and RHCP in $-z$ direction at lower and higher resonating frequencies, respectively.

Figure 13 depicts surface current distribution at 2.45 GHz lower band. As shown in Figs. 13(a) and (b), current in ground plane rotates in clockwise direction, yielding LHCP polarization.

(a)   (b)
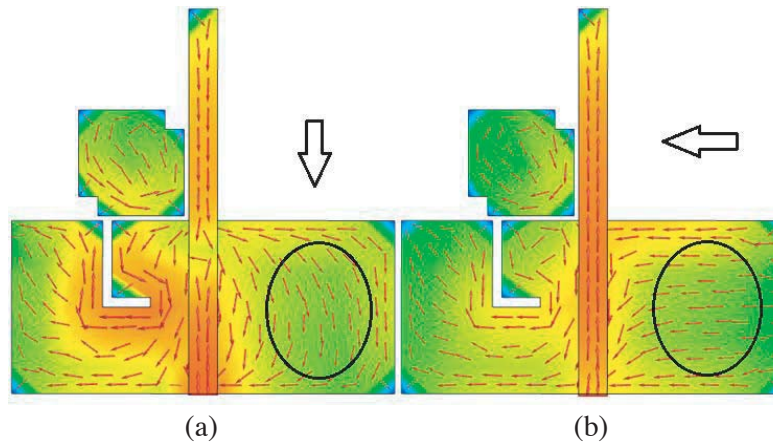
Figure 13. Current distribution at 2.45 GHz (a) 0° and (b) 90°.

Figures 14(a) and (b) show surface current at 5.9 GHz for 0° and 90°. The surface current is in anticlockwise direction yielding right-hand circular polarization (RHCP). However, as parasitic patch is beneath the monopole, it exhibits RHCP in $-Z$ direction and LHCP in $+Z$ direction as shown in Figs. 12(c) and (d), respectively.


(a)   (b)
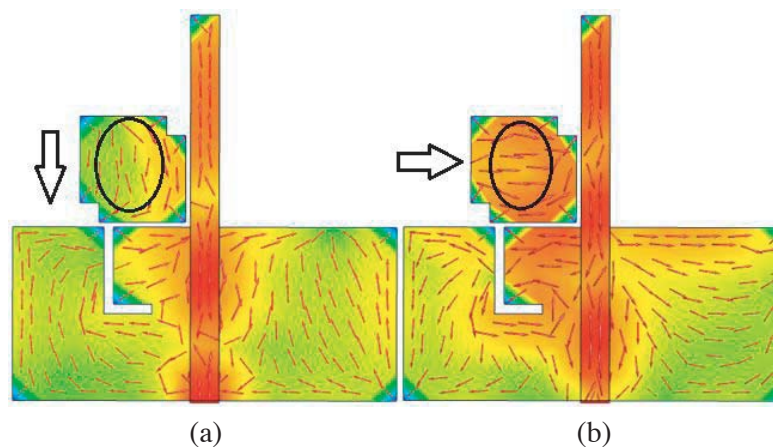
**Figure 14.** Surface current at 5.9 GHz (a) 0° and (b) 90°.

4.2. Measured Results and Comparison

The designed antenna is fabricated and tested using R & S ZVL vector network analyzer. Fig. 15 shows the comparison of measured return loss characteristics with simulated result. Fig. 16 shows photographs of the fabricated prototype.

Figure 17 shows measured return loss characteristics with experimental setup shown in inset. The measured results show impedance bandwidth of 19.43% and 12.73% at center frequency of 2.47 GHz
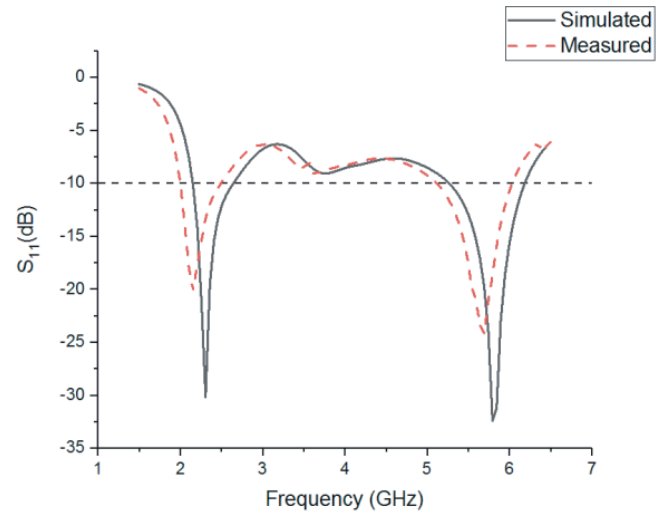
Figure 15. Simulated and measured return loss of dual band CP antenna.

(a)   (b)
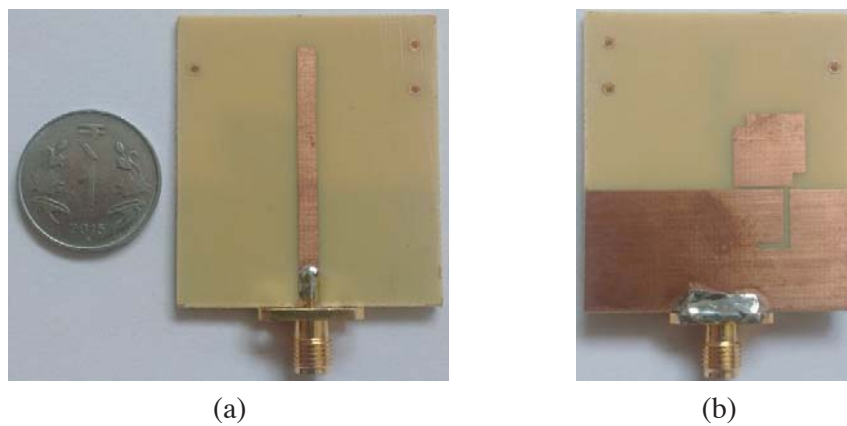
Figure 16. Fabricated prototype, (a) top side, (b) bottom side.

Figure 17. Measured return loss and experimental setup.

and 5.97 GHz for WLAN and Vehicular band, respectively. Fabrication losses result in slight downside in the measured results at 3.02 GHz. The measured results are in close agreement with simulated ones.

5. CONCLUSION

In this research work, a dual-band CP microstrip patch antenna for WLAN and vehicular communication is presented. The antenna design is simple and fabricated using a low cost substrate. The antenna exhibits dual-band CP response with 20.45% and 15.73% simulated, and 19.43% and 12.73% measured impedance bandwidths. The antenna also offers wide axial ratio bandwidths of 6.84% and 14.16%. The transmission line equivalent circuit for proposed antenna is designed and discussed. The simulated and measured results are in close agreement with each other showing that the designed antenna can be a good candidate for WLAN and vehicular communication applications.

ACKNOWLEDGMENT

REFERENCES

1. IEEE Standard for Information Technology — Telecommunication and Information Exchange between Systems — Local and Metropolitan Area Networks-Specific Requirements; Part 11: Wireless LAN Medium Access Control (MAC) and Physical Layer (PHY) Specifications; Amendment 6: Wireless Access in Vehicular Environments, IEEE Std. 802.11p, Jul. 2010.
2. Uhlemann, E., "Connected-vehicles applications are emerging," *IEEE Vehicular Technology Magazine*, 25–28, Mar. 2016.
3. Viriyasitavat, W., M. Boban, H.-M. Tsai, and A. V. Vasilakos, "Vehicular communications-survey and challenges of channel and propgation modes," *IEEE Vehicular Technology Magazine*, 55–66, Jun. 2015.
4. Wong, H., K. K. So, and X. Gao, "Bandwidth enhancement of a monopolar patch antenna with V-shaped slot for car-to-car and WLAN communications," *IEEE Transactions on Vehicular Technology*, Vol. 65, No. 3, 1130–1136, Mar. 2016.
5. Hao, H., J. Li, D. Huang, and W. Luo, "Design of hexagon microstrip antenna for vehicle-to-vehicle communication," *The Journal of China Universities of Posts and Telecommunications*, Vol. 23, No. 4, 69–76, 2016.
6. Mondal, T., S. Samanta, R. Ghatak, and S. R. Bhadra Chaudhari, "A novel tri-band hexagonal microstrip patch antenna using modified Sierpinski fractal for vehicular communication," *Progress In Electromagnetics Research C*, Vol. 57, 25–34, 2015.
7. Ijiguchi, T., D. Kanemoto, K. Yoshitomi, K. Yoshida, A. Ishikawa, S. Fukagawa, N. Kodama, A. Tahira, and H. Kamaya, "Circularly polarized one-sided directional slot antenna with reflector metal for 5.8-GHz DSRC operations," *IEEE Antennas and Wireless Propagation Letters*, Vol. 13, 778–781, 2014.
8. Lee, D.-H., D.-W. Chung, E.-G. Kim, and S. Pyo, "Circular polarization agile microstrip antenna for wireless access in vehicular environments," *Microwave and Optical Technology Letters*, Vol. 56, No. 10, 2310–2313, 2014.
9. Leonardi, O., M. G. Pavone, G. Sorbello, A. F. Morabito, and T. Isernia, "Compact single layer circularly polarized antenna for short range communication system," *Microwave and Optical Technology Letters*, Vol. 56, No. 8, 1843–1846, 2014.
10. Sim, C. Y. D. and B. H. Yang, "A single layer dual-band CP microstrip antenna for GPS and DSRC applications," *Journal of Electromagnetic Waves and Applications*, Vol. 22, 529–539, 2009.

11. Donelli, M. and F. Robol, "Circularly polarized monopole hook antenna for ISM band systems," *Microwave and Optical Technology Lettters*, Vol. 60, 1452–1454, 2018.

12. Donelli, M., T. Moriyama, and M. Manekiya, "A compact switched-beam planar antenna array for wireless sensors operating at Wi-Fi band," *Progress In Electromagnetic Research C*, Vol. 83, 137–145, 2018.

13. Donelli, M. and P. Febvre, "An inexpensive reconfigurable planar array for Wi-Fi applications," *Progress In Electromagnetic Research C*, Vol. 28, 71–81, 2012.

14. Gao, S., Q. Luo, and F. Zhu, *Circularly Polarized Antennas*, John Wiley & Sons, Ltd., 2004.

15. Altair's Hyperworks CAD FEKO, Altair Engineering Inc., USA.

16. Pozar, D. M., *Microwave Engineering*, John Wiley & Sons, Ltd., 2008.

17. Moradikordalivand, A., T. A. Rahman, S. Ebrahimi, and S. Hakimi, "An equivalent circuit model for broadband modified rectangular microstrip-fed monopole antenna," *Wireless Personal Communication*, Vol. 77, 1363–1375, 2014.

18. Garg, R., P. Bhartia, I. Bahl, and A. Ittipiboon, *Microstrip Antenna Design Handbook*, Artech House, Norwood, MA, 2000.

19. Ansari, J. A., S. K. Dubey, and A. Mishra, "Analysis of half E-shaped patch for wideband application," *Microwave and Optical Technology Letters*, Vol. 51, No. 6, 1576–1579, 2009.